

# Low Cycle Fatigue Behaviour of Multi-joint Sample in Mechanical Testing

C.P. Hunt<sup>1</sup>, O. Thomas<sup>1</sup>, D. Di Maio<sup>1</sup>, E. Kamara<sup>2</sup>, H. Lu<sup>2</sup>

1. National Physical Laboratory,  
Queens Road, Teddington, Middlesex TW11 0LW, UK
2. University of Greenwich, Park Row, Greenwich, London, SE10 9LSUK

## Abstract

This paper explores the behaviour of a copper test vehicle with multiple reflowed solder joints, which has direct relevance to ball grid arrays (BGA) and high density interconnect structures. The paper explores the relative stress conditions on the distributed joints and the sensitivity to ball joint shape. The joints were exposed to isothermal fatigue, which was produced by a mechanical load that induced a cyclic shear stress across all the joints. The same structures were modelled using finite element analysis. The loading response distribution profile through the joints was analysed. The regions of likely failure were identified to be along the shear band and at the stress concentration areas in the corners of the joints. Failure of the individual joints was analysed by quantifying the accumulated creep strain per cycle. Solder joint models of three different shapes were investigated: rectangular, convex and concave shapes. This analysis has shown that less damage is found in concave shaped joints, indicating that BGAs would have more damage than the rectangular joints tested here. Results have also shown that more damage occurs in the outer joints as a vertical component appears due to a turning moment on the copper test vehicle. This behaviour could affect the external joints of large components, where the same vertical stress component may arise due to the differential CTE of the PCB and BGA component.

## Introduction

Mechanical testing of solder joints in a cyclic mode provides materials' data as the solder experiences fatigue. These data can be informative in discriminating between various solders, but can additionally be combined with finite element modelling in characterising behaviour. This paper investigates the properties of a multi-joint sample, studying the properties as the number of joints was increased. A motivation for this work was the relevance of this structure to area array packages. The popular Ball Grid Array (BGA) package offers high interconnection density, easy assembly, and low thermal resistance. Typically, a square array of solder balls connect a laminate substrate and a semiconductor die. Because of their geometry, the ball-shaped solder joints in BGAs are not able to easily deform to accommodate thermal-mechanical and other stresses [1]. Due to the Coefficient of Thermal Expansion (CTE) mismatch between Printed Circuit Board (PCB) substrate and the package, solder joints experience a cyclic strain in temperature varying conditions that induce fatigue in the solder joints and other parts of the assembly [1,2]. In this paper, we shall focus on isothermal fatigue testing of specimens containing multiple solder joints. The loading conditions on solder joints are similar to those found in BGAs that are subject to thermal-mechanical loading. The aim of the work is to establish an effective low cost test system that can be used for the evaluation of solder alloys that are used for BGAs, and to provide material data that can be used in physics-of-failure based reliability prediction for BGA or other similar devices with solder interconnects.

## Experimental Procedure

Solder interconnect samples with multiple joints were fabricated from copper coupons of size 51×6×1 mm. A low speed diamond saw was first used to produce a 0.3 mm cut running centrally along almost the entire length of the coupon. This slit was placed over a jig comprising an oxidised stainless steel shim with a specified number of slots corresponding to the size and number of joints required in the sample. Before soldering, this space was filled in excess with the desired solder paste. In this study, 96.5Sn3.0Ag0.5Cu lead free solder was used. The jig was then placed onto a hot plate for solder reflow, after 5 seconds into the reflow process, the jig was removed from the hot plate and placed on a cold metallic surface to cool such that the time above the reflow temperature was between 10 to 30 seconds. Abrasive paper was used to remove excess solder and slots were cut in the sample (Figure 1) such that when pushed/pulled, a shear force is applied to the solder joints. Samples with 1 to 8 joints were prepared using this procedure and these are referred to as M1-M8.

The samples were tested by applying isothermal cyclic displacement loading using the Interconnect Properties Testing Machine (IPTM), an instrument described in detail elsewhere [3, 4]. The ends of the samples were clamped and pulled/pushed along the length to produce cyclic deformation in solder joints. A load cell was used to monitor the supported force and laser displacement sensors were used to measure the distance between the fixed and moving stages of the instrument. The displacement was controlled through the thermal expansion of a stainless steel tube connected to the moving stage. As such, the machine can accurately control the strain applied to the sample, whilst measuring the supported

load. In addition, a camera with microscope attachment was placed over the sample to take time-lapse photos of the sample during the test.

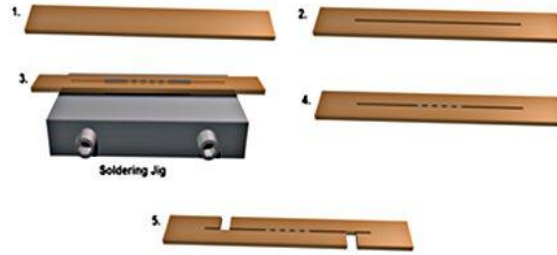


**Figure 1: Illustration of sample preparation.**

The displacement range applied was  $-30$  to  $30\mu\text{m}$ , and the ramp rate was  $10^{-7}\text{m/s}$  and the dwell time was 5 minutes, producing a cycle time of 30 minutes (see Figure 2). With increasing number of solder joints, the supported force load increases and the strain in the copper also increases, whilst the strain in the solder joints is reduced as a result. To produce a controlled strain in samples with different number of solder joints, the compliance of the copper needs to be taken into account when applying the displacement. To apply this correction, a copper coupon with the same geometry but without solder joints was first tested in the IPTM. Since the supported force is in the elastic region of the copper, it is possible to correct the solder joints tests in real time with the maximum applied displacement adjusted to take into account the extra displacement in the copper. The applied displacement is obtained from Eqn 1.

$$d(t) = w(t) + kF(t) \quad (1)$$

where  $d(t)$  is the displacement applied at time  $t$ ,  $w(t)$  is the waveform displacement required,  $F(t)$  is the force and  $k$  is the experimentally found compliance. With this correction, the same displacement waveform could be applied to each of the different number of joint samples.

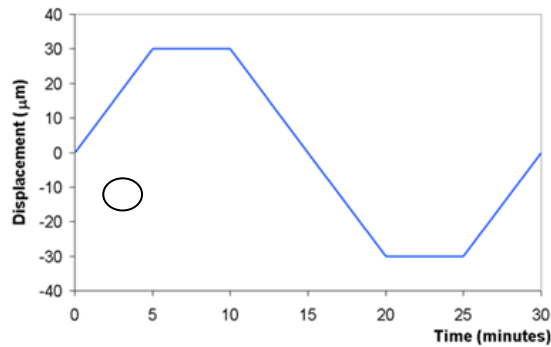


**Figure 2: The required displacement waveform.**

### Modelling Procedure

The tests have been simulated using Finite Element Analysis(FEA) software ANSYS Mechanical APDL [6]. Figure 3 shows the model of a sample with 6 solder joints.

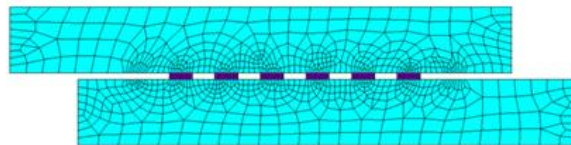


**Figure 3: FEM meshing of a 6 joints sample.**

The elastic material properties used for the simulations are as shown in Table 1. The loading profile is the same as the one in the experiment (Eqn. 1 and Fig. 2). Since we are dealing with low cycle fatigue, the effect of creep is significant and

should be taken into account. In this study the Garofalo's creep model [5] was used to simulate the effect of creep in solder specimens and the creep strain rate equation is shown in Eqn. 2.

$$\dot{\epsilon}_{cr} = c_1 [\sinh(c_2 \sigma)]^{c_3} \exp\left(-\frac{c_4}{T}\right) \quad (2)$$

where  $c_1, c_2, c_3$  and  $c_4$  are material constants,  $T$  is the temperature,  $\sigma$  is the effective stress and  $\epsilon_{cr}$  is the creep strain.

**Table 1: Material properties. E and  $\nu$  are Young's modulus and Poisson's ratio respectively.**

Material	E (GPa)	$\nu$
Sn 3.0Ag 0.5Cu	50	0.4
Copper	120	0.33

In the current experiments, solder joints are approximately cuboid in shape. In order to understand the effects of geometry on the stress state in solder joints, three different solder interconnect shapes are modelled: rectangular, convex and concave shapes (illustrated in Fig. 4). Each solder joint is modelled using 400 ANSYS SOLID185 elements.

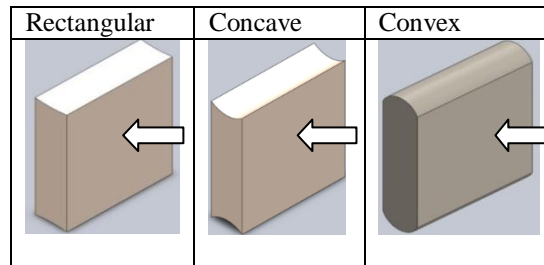


**Figure 4: Solder joint shapes investigated. The arrows indicated where the attachment will be between the solder and copper**

To predict the damage caused by cyclic loading on the solder joints and hence their lifetime, the volume weighted accumulated equivalent creep strain (ANSYS output variable NLCREP) per cycle  $\epsilon_{acc}$  was obtained. A typical accumulated equivalent creep strain value is shown in Fig. 5 for the first three cycles of loading. The value of  $\epsilon_{acc}$  was not a constant but from the third cycle the change becomes very small.

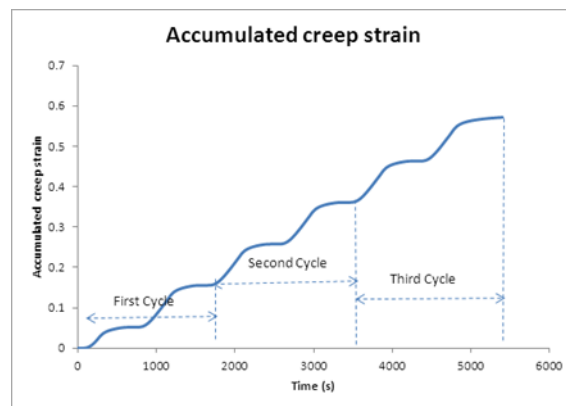


**Figure 5: Accumulated creep strain over three cycles for five sample solder joint**

$\varepsilon_{acc}$  is a measure of the damage in a solder joint and it can be linked to the solder joint lifetime through an empirical Coffin-Manson type lifetime model. In this work, the lifetime model used to calculate the lifetime of solder joint is as given by Syed [7]:

$$N_f = (0.0513\varepsilon_{acc})^{-1} \quad (3)$$

### Results and Discussions

Each sample was mechanically cycled until the load dropped to 50% of the maximum supported load. Figure shows how the load drops of for 3 M5 samples. The variability in the rate at which the load drops for samples of the same type is mainly caused by the statistical nature of the fatigue process [8], but also by unavoidable voids and defects in the samples, and small geometrical differences. Optical micrographs of the fatigue damage produced in some of the samples are shown in Fig. 7.

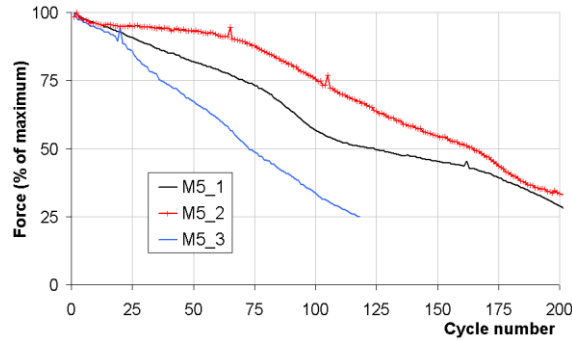


Figure 6: Force drop (as % of maximum) vs cycle number for the sample with five joints.

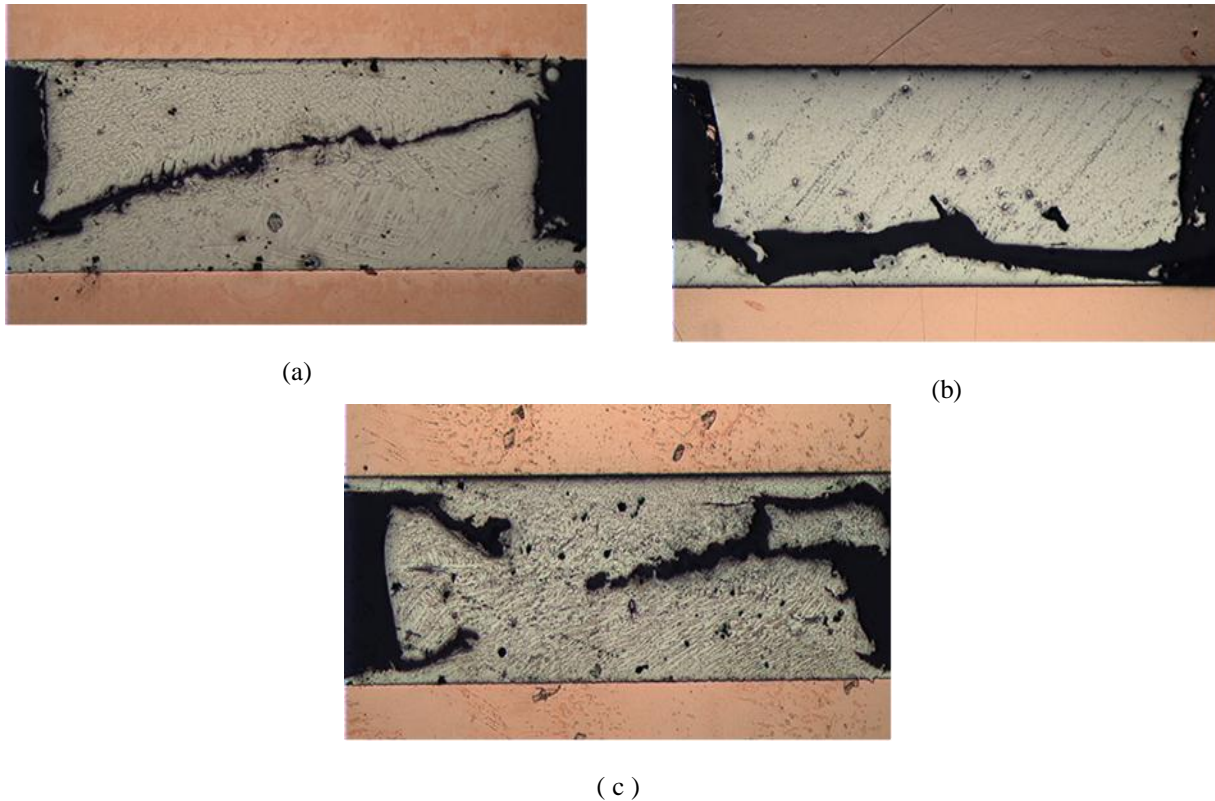


Figure 7: (a) Crack in the central joint of a M5 sample; (b) crack in the third joint of a M8 sample (c) multiple cracks in an M5 sample and crack along the interface.

In the simulation, stress and strains are obtained. Fig. 8 shows the effective stress as a function of time at the corner of one of the outermost solder joint in a M5 sample. It shows that the stress is highest just before the onset of the dwell periods. Figure 9 shows a snapshot of the Von Mises and shear stress distribution in the M5 sample at 2088s. The maximum stress is located at the solder-copper interface of the corner solder joints. Because of the stress relaxation, the stress level in solder joints exhibits much less inhomogeneity than in copper. The shear stress is concentrated in solder joints but it is not uniformly distributed. As the figure shows, the copper parts bend slightly under the loading and deformation in solder joint is therefore not pure shear, and stress states are expected to vary from one joint to another. Deformation in the perpendicular direction is greatest for the outermost solder joints due to the bending in the copper. This situation does have parallels to what will happen in BGA solder joints under thermal-mechanical loading. Another interesting phenomenon that can be observed is diagonal shear band, in the edge solder joints in particular.

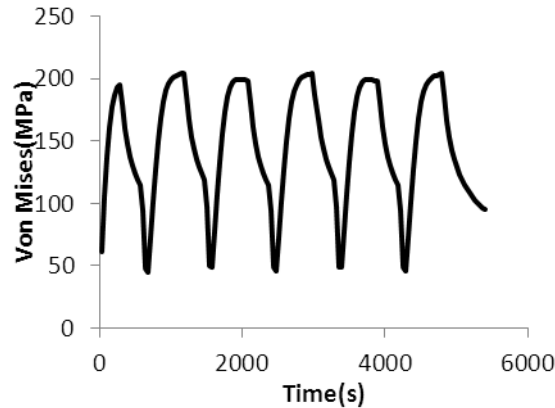


Figure 8: Von Mises stress at the corner of the edge solder joint of a 5-joint model (M5).

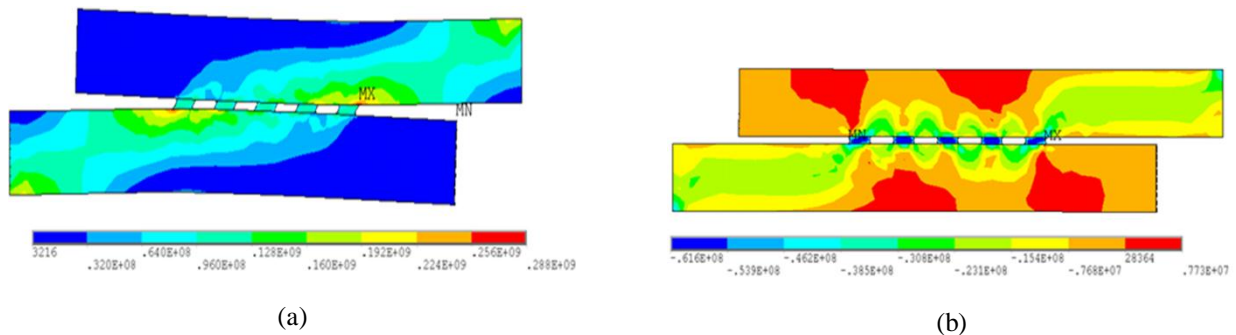
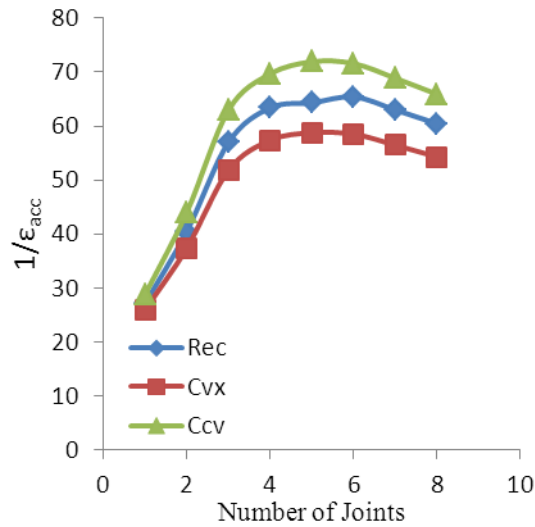


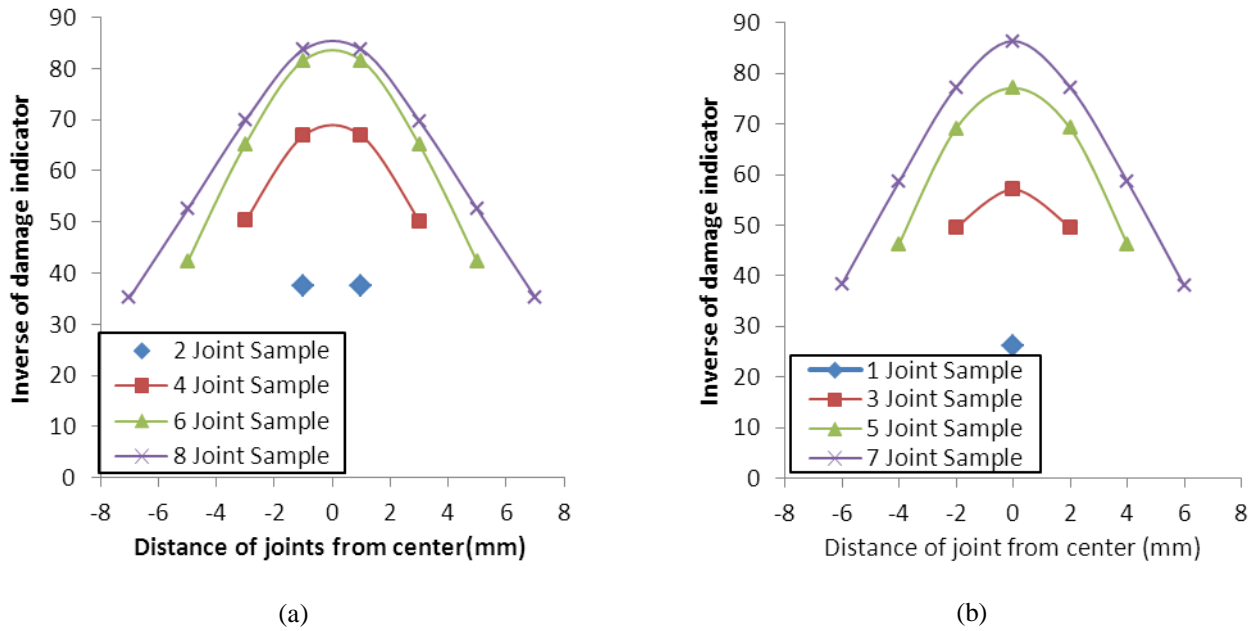
Figure 9: (a) Von Mises Stress and (b) Shear Stress XY in a modelled 5 joint sample at the start of the first dwell at 30  $\mu\text{m}$  displacement. Displacement in image (a) has been magnified 20 times.

Fig. 10 shows how the three different shapes investigated affect the calculated lifetime for the different number of joints investigated. The results suggest that the convex shapes will have less damage and hence longer lifetime than that of the concave and rectangular shapes.



**Figure 10:  $1/\epsilon_{acc}$  vs. number of joints in the sample for the rectangular (Rec), Convex (Cvx) and Concave (Ccv) solder joint shapes.**

In Fig. 11, the values of the inverse damage, i.e.  $1/\epsilon_{acc}$ , for each individual solder joints are plotted. The results show that outermost solder joints suffer more damage than internal ones and will therefore fail first.



**Figure 11: Modelled joint inverse damage for (a) even and (b) odd number of joints samples.**

Fig. 11 also shows that in general, samples with different number of joints have different average damage. This is confirmed by Fig. 12 where the average damage is shown for samples with 1 to 8 joints. The result indicates that the single joint sample will be the most damaged of all the multi-joint models and that the least damaged will be the M5 sample, and M4 and M6 showing similar results.

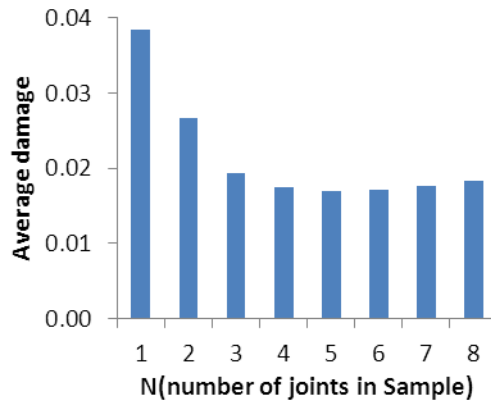


**Figure 12: Average damage in samples with N number of joints.**

### Discussion

The experimental results for the number of cycles required to reach 10%, 20% and 50% of load drop from the maximum load, is plotted in Figure 13 against the number of joints per sample. The relationship between the number of joints and the cycles to reach a pre-defined failure is not that clear but it does show that the sample with the longest lifetime is the M5, which is consistent with the simulation result.

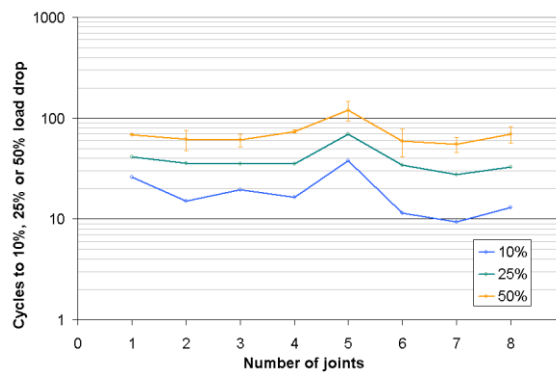


**Figure 13: Cycles to 10%, 20% and 50% vs number of joints in sample. Error bars on the 50% load drop data represent the repeatability observed from testing on average 3 samples for each number of joints.**

Using the time-lapse photography technique, 4 main different types of failure/crack propagation mechanisms were identified. Type 1 consists of a crack that runs diagonally across the sample as in Fig. 7(a). Type 2 consists of a crack that runs parallel to the interface, as in Fig. 7(b). Type 3 consists in a crack along or very close to the interface (Fig. 7(c)). This is similar to what Lai *et. al* have found in their study [9]. Finally, type 4 is a surface damage that causes the solder to appear darker but without any visible crack.

Crack initiation did not occur at a single point; sometimes cracks initiated in one place, sometimes in several places, with multiple cracks growing and combining as the sample became more damaged (see Fig. 6(c)). Cracks propagated in all joints almost simultaneously, with minimal changes in crack propagation rate between different joints. However, a tendency for the outer joints to fail first compared to the inner joints was observed, which is consistent with simulation results. A number of the samples contained voids, but it was not possible to establish a correlation with crack propagation and the presence of voids, as established by Yunus *et al.* [10].

Computer simulations have shown solder joints experience both shear and normal stress of appreciable magnitude, confirming that the stress states in the multi-joint test samples are similar to those in BGA solder joints. Samples with 5 solder joints were predicted to have the longest lifetime, and this was supported by the experimental results. The most significant difference between the modelling results and the experimental results was that the experimental results for one or eight solder joints were not the ones with the shortest lifetime. This needs more investigation. In future work, lifetime models will be derived based on experiments on the solder joint specimens.

### Conclusions

- Fabrication and testing of a multi-joint sample has been demonstrated.

- Modelling has predicted that joint shape will have an effect on fatigue, with the natural convex shape having the superior performance.
- Experiments and modelling have shown that damage occurs more in joints as they become further from the centre point.
- Modelling has shown there is a turning moment, and that a vertical component force appears of increasing amplitude with distance from the centre of the component. This force, normal to the shear direction, is consistent with these joints failing more rapidly.
- This behaviour could affect the external joints of large BGA components, where the same vertical stress component may arise due to the differential CTE of the PCB and component.

### Acknowledgements

The authors acknowledge the financial support of the National Measurement Office , and the IeMRC, EPSRC.

### References

- [1] Moore, T.D., and J.L. Jarvis. "Failure analysis and stress simulation in small multichip BGAs." *IEEE Transactions on Advanced Packaging* 24, no. 2 (May 2001): pp216-223.
- [2] Zhang, Bo, Han Ding, and Xinjun Sheng. "Reliability study of board-level lead-free interconnections under sequential thermal cycling and drop impact." *Microelectronics Reliability* 49, no. 5 (May 2009): pp530-536.
- [3] D. Di Maio, O. Thomas, M. Dusek & C. Hunt, "Novel Testing Instrument for Lead-Free Solder Characterization", *IEEE Transactions on Instrumentation and Measurements*, In Press.
- [4] D. Di Maio, C. Murdoch, O. Thomas, C. Hunt, "The Degradation of Solder Joints under High Current Density and Low-Cycle Fatigue", 2010 11th International Thermal, Mechanical & Multi-Physics Simulation, and Experiments in Microelectronics and Microsystems (EuroSimE), pp1-6
- [5] Hongtao Ma. "Constitutive models of creep for lead-free solders." *J Mater Sci* (May 2009) 44:pp3841-3851
- [6] ANSYS Mechanical APDL 12.0.1, ANSYS Inc. 2009
- [7] A. Syed, "Accumulated Creep Strain and Energy Density Based Thermal Fatigue Life Prediction Models for SnAgCu Solder Joints", Corrected versions of the paper presented in the 54th Electronic Components and Technology Conference, Las Vegas, USA, 1-4 June, 2004, pp. pp737-746
- [8] Palmer, M A. "Thermomechanical Fatigue Testing and Analysis of Solder Alloys." *Stress: The International Journal on the Biology of Stress* 122, no. March (2000): pp48-54.
- [9] Lai, J.K.L., K.C. Hung, Y.C. Chan, and P.L. Tu. "Comparative study of micro-BGA reliability under bending stress." *IEEE Transactions on Advanced Packaging* 23, no. 4 (2000): pp750-756.
- [10] Yunus, M, K Srihari, J Pitarresi, and a Primavera. "Effect of voids on the reliability of BGA/CSP solder joints." *Microelectronics Reliability* 43, no. 12 (December 2003): pp2077-2086.